

A high temperature superconductor dc SQUID planar gradiometer measurement system for routine inspections

M I Faley^{1,2}, U Poppe¹, V Yu Slobodchikov², Yu V Maslennikov²
and K Urban¹

¹ Institut für Festkörperforschung, Forschungszentrum Jülich GmbH, D-52425 Jülich, Germany

² Institute of Radio Engineering and Electronics, 101999 Moscow, Russia

Received 4 December 2003

Published 6 April 2004

Online at stacks.iop.org/SUST/17/S301 (DOI: 10.1088/0953-2048/17/5/041)

Abstract

We have developed a high temperature superconductor (HTS) dc SQUID gradiometric measurement system for routine applications in non-destructive evaluations. Low values of the white flux noise and white field gradient noise were measured for gradiometers operating at 77 K. Low frequency noise was suppressed using an ac bias technique, even in a magnetically unshielded environment. First-order planar dc SQUID flip-chip gradiometers were used in the measurement system for stable operation under electromagnetically noisy conditions. A synchronous filter was employed to remove all harmonic components of parasitic line frequency interference. This improved the resolution of the system in a typical laboratory or industrial environment showing strong magnetic gradients of the line frequency signal due to nearby metallic constructions. Test scans of contaminations with magnetic particles were performed.

1. Introduction

For the development and routine production of sensitive magnetic measurement systems, permanent control of constructional parts of the system for magnetic contamination is necessary. Magnetic contamination degrades the noise properties of the system and has to be avoided. One of the main sources of magnetic contamination is, e.g., workshop dust sometimes containing a few tiny ($\sim 100 \mu\text{m}$) particles of magnetic alloys (Fe, Co, Ni, etc, compounds). These particles can be hidden under the surfaces of the parts and be easily passed by during optical inspection.

The measurement system for such routine inspections should provide the necessary resolution at a distance of a few centimetres from the magnetic particles, but should also not require too much care to maintain its own functions in a magnetically unshielded laboratory environment. The magnetic field resolution achieved by high temperature superconductor (HTS) dc SQUID sensors [1] is sufficient for many applications. The planar HTS dc SQUID flip-chip gradiometer HTG-10R [1] is very well suited to tasks where the object-to-sensor distance ranges from about 1 cm to about 10 cm.

The standard HTS sensors are optimized for operation with liquid nitrogen coolant. Liquid nitrogen is much easier to handle compared to liquid helium, which is required for the cooling of low temperature superconductor SQUIDs. Also the cryogen hold time of a mature liquid nitrogen system is about five times longer than the cryogen hold time of a liquid helium system.

SQUIDs are quite sensitive to radio-frequency (rf) and microwave interference [2] (such as mobile phone signals) and therefore usually need to be shielded microwave-tight. Relatively high magnetic noise of a typical laboratory or industrial environment significantly complicates the operation and degrades the resolution of the SQUID system unless a well-balanced hardware gradiometric sensor arrangement is used (see, e.g., [3]). Additionally, the residuals of line frequency interference and its harmonics should be removed by a proper filtering.

In this work we report on a HTS dc SQUID gradiometric system suitable for routine magnetic evaluation inspections. The system is based on a HTS dc SQUID planar first-order gradiometer HTG-10R [1] and has been used for more than a year in the laboratory without magnetic shielding.

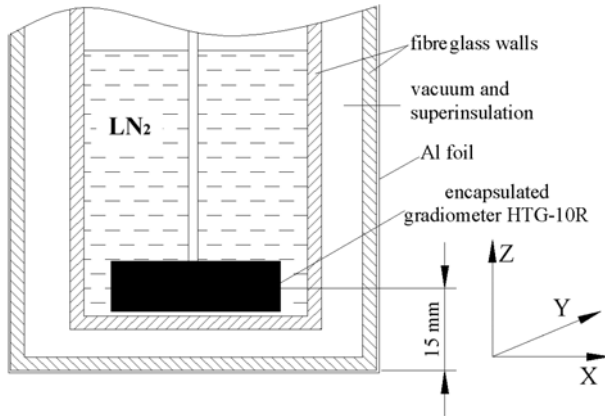


Figure 1. A schematic view of the HTG-10R gradiometer position in the cryostat.

2. Experimental details

The $\text{YBa}_2\text{Cu}_3\text{O}_{7-x}$ and $\text{PrBa}_2\text{Cu}_3\text{O}_{7-x}$ *c*-oriented films of the gradiometer were deposited by a high oxygen pressure dc sputtering technique [4]. The HTS Josephson bicrystal junctions for the dc SQUIDs were prepared on symmetric 24° bicrystal $\text{SrTiO}_3(100)$ substrates. The junctions had a width ranging from 0.4 to 1 μm , a normal state resistance of about 10 Ω , and a critical current density of about $2 \times 10^4 \text{ A cm}^{-2}$ at 77.4 K [5]. The $I_c R_n$ product of the junctions was about 400 μV at 77 K. The junctions were prepared by optimized conventional photolithography with AZ photoresist, 0.3 μm UV-light exposure, and Ar ion milling. The application of the submicrometre-width bicrystal Josephson junctions has increased the modulation voltage V_{pp} of the gradiometer up to 80 μV ($\partial V / \partial \Phi \approx 250 \mu\text{V} / \Phi_0$) at 77.4 K in comparison to the gradiometer with wider junctions.

The measurements were performed with the encapsulated sensors immersed in liquid nitrogen (LN_2) in a fibre-glass epoxy cryostat (see figure 1). The plane of the HTG-10R gradiometer was oriented horizontally (*x*, *y*-plane). The 25 mm multilayer flux transformer of the planar gradiometer was prepared by a technique described in [5]. The $\text{PrBa}_2\text{Cu}_3\text{O}_{7-x}$ insulation layer between the windings of the multiturn input coil and the return strip prevents superconducting shorts and provides a normal conducting shunt between superconducting layers to avoid high frequency resonances in the multiturn coil structure [6].

The cryostat (see figure 2) was wrapped microwave-tight in an Al foil. The foil had a thickness of $d = 10 \mu\text{m}$ and was grounded via the rf shield of the SQUID electronics. The Nyquist noise B_N of the Al foil at the gradiometer position was estimated to be about 20 fT $\text{Hz}^{-1/2}$ according to the following equation (see [7] and [8]):

$$B_N = \frac{1}{2} \mu_0 \sqrt{\frac{kT\sigma}{2\pi} \frac{d}{z(z+d)}}, \quad (1)$$

where $\sigma = 3.6 \times 10^7 \text{ S m}^{-1}$ is the conductivity of Al and $z = 15 \text{ mm}$ is the distance between the foil and the sensor (see figure 1). This distance is mainly limited by the thickness of the encapsulation. The cold-warm distance at the cryostat bottom is about 10 mm. The latter is necessary to provide the

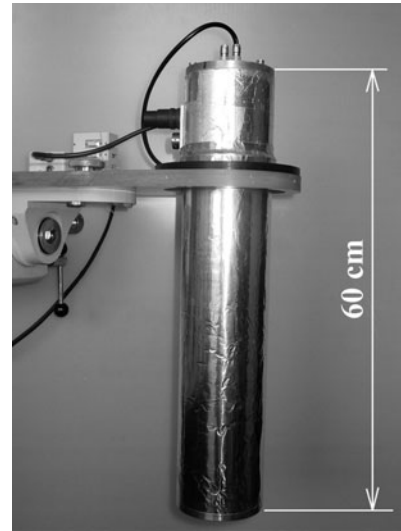


Figure 2. An rf-shielded LN_2 cryostat used for operation with the planar HTG-10R gradiometer in a magnetically unshielded environment.

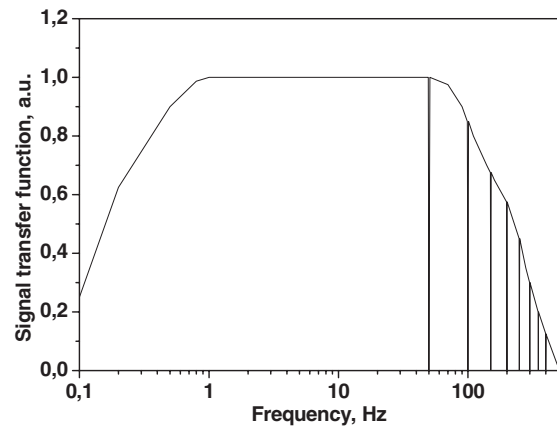


Figure 3. The signal amplitude transfer function of the 50 Hz synchronous filter.

present cryogen hold time of the 1.5 l LN_2 cryostat with an installed gradiometer insert of about ten days.

The output signal of the SQUID electronics was filtered by a synchronous 50 Hz filter³. The filter signal amplitude transfer function is presented in figure 3. Strong notch-type suppressions by a factor of about 1000 with a 1 Hz bandwidth around the 50 Hz interference and its harmonics were observed.

3. Results

The system noise spectra are presented in figure 4. The dashed curve represents a spectrum of the unfiltered gradiometer signal measured in a μ -metal shield around the cryostat. The system showed white gradient noise below 40 fT $\text{cm}^{-1} \text{ Hz}^{-1/2}$ at frequencies above 100 Hz. The noise increased to about 200 fT $\text{cm}^{-1} \text{ Hz}^{-1/2}$ at 1 Hz.

Outside the magnetic shield the environmental magnetic noise, such as a low frequency drift, the effect of vibrations,

³ CRYOTON Co. Ltd, Solnechnaya Avenue 12, Troitsk, Moscow Region, 142190, Russia.

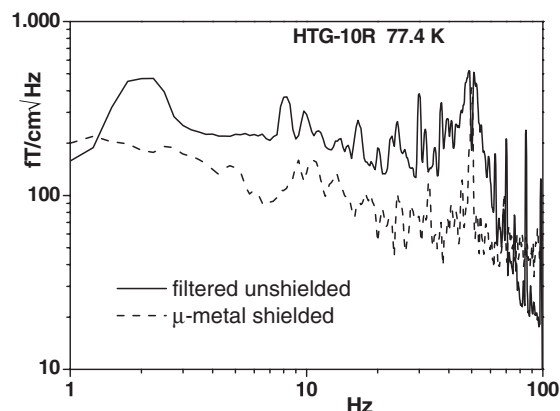


Figure 4. System noise spectra of the planar gradiometer HTG-10R measured unfiltered in a μ -metal shield (dashed curve) and filtered without a magnetic shield (solid curve).

and harmonics of the 50 Hz interference, was observed. Due to the gradiometer configuration a significant part of the environmental magnetic noise is automatically subtracted from the output signal. For example, the typical peak-to-peak amplitude of the 50 Hz magnetic signal in the laboratory was about 70 nT. The 50 Hz peak-to-peak output signal of the system with the HTG-10R planar gradiometer sensor was measured as about 50 pT cm^{-1} . This balance value (~ 1400) was achieved at a typical scanning frequency of about 1 Hz by a correction performed with a small piece of permalloy foil fixed on the cryostat surface at a distance of about 10 cm from the gradiometer. Such balance correction compensates for the disbalance of the gradiometer due to an effect of the superinsulation, Al foil, and other metal parts in the vicinity of the gradiometer.

The solid curve in figure 4 represents the spectrum of the filtered output signal obtained without a magnetic shield. The application of the synchronous 50 Hz filter completely removed the 50 Hz interference signal and all its harmonics. This significantly improved the signal-to-noise ratio of the system. Also some reduction of the noise at frequencies below 1 Hz and above 70 Hz was observed in accordance with the filter transfer function presented in figure 3.

Routine inspections of constructional parts (fibre-glass parts, cryostat, sample holders, cables, etc) were performed in a magnetically unshielded laboratory environment. The parts were held in the hand during the scan under the bottom end of the cryostat. Such scans provide the easiest and fastest test of the parts for the presence of small magnetic particles.

It was observed that the sensitivity of the system to the magnetic contaminations is significantly better than those of other (e.g., the flux-gate based one) systems available in the laboratory. Magnetic particles with diameters down to a few micrometres were routinely detected and localized with about 1 mm spatial resolution. Also magnetic moments of small dipoles can be determined.

Typical examples of test measurements are presented in figures 5 and 6. In the first case, the magnetic dipole moment of the magnetic particle was oriented vertically along the cryostat axis (z -axis). In the second case, the magnetic moment is oriented parallel to the baseline of the gradiometer and the scan direction. The baseline of the gradiometer was oriented

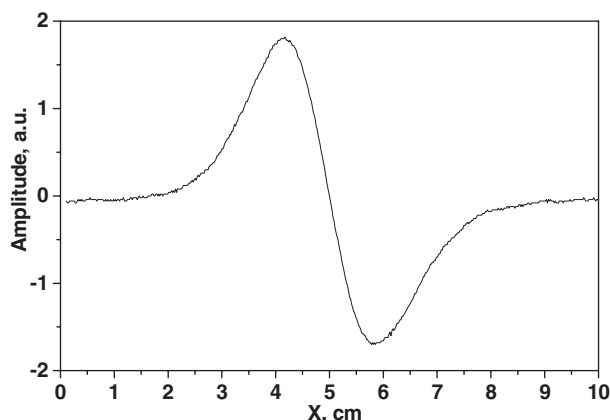


Figure 5. An example of the measurement in the case where the magnetic moment of the particle was parallel to the z -axis.

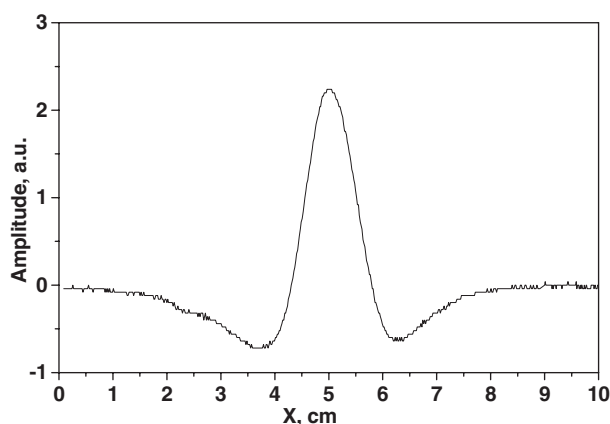


Figure 6. An example of the measurement in the case where the magnetic moment of the particle was parallel to the x -axis.

along the x -axis. In the case of very soft magnetic material of the particle (e.g., amorphous permalloy) the curves observed may depend on the orientation of the system relative to the direction of the Earth's magnetic field.

4. Discussion

The quantitative analysis of the scan data can be performed on the basis of the magnetic field distribution \vec{B} (T) generated by the magnetic dipole:

$$\vec{B} = \frac{\mu_0}{4\pi} \left[\frac{3(\vec{P}\vec{r})\vec{r}}{r^5} - \frac{\vec{P}}{r^3} \right], \quad (2)$$

where \vec{P} (A m^2) is the magnetic moment of the dipole and \vec{r} (m) is the distance from the dipole to the measurement point.

Nearly spherical magnetic inclusions can have a specific magnetic moment of about $0.07 \text{ A m}^2 \text{ g}^{-1}$ in the case of, e.g., SmCo_5 . A magnetic particle about $10 \text{ }\mu\text{m}$ in diameter has a mass of about 7 ng and, correspondingly, a magnetic moment $P \sim 0.5 \text{ nA m}^2$. The maximal magnetic field of such particle at a distance of 15 mm is about 30 pT. The magnetic field gradient $\partial B_z / \partial x$ (T m^{-1}) at this distance from the particle is about $0.64\mu_0 P / \pi z^4 \sim 25 \text{ pT cm}^{-1}$. If we assume a measurement bandwidth of about 100 Hz and a

signal-to-noise ratio of about 10 for such measurements, then according to the noise data (see figure 4) the system can resolve the gradient signal from such particles of about 30 pT cm^{-1} , which is in reasonable agreement with the observed values. Steel magnetic particles typically have about ten times less remanent specific magnetic moment compared to SmCo_5 and, correspondingly, about ten times greater minimum value for detectable masses.

In accordance with equation (2) the scan data curve, shown in figure 5, can be described by the following dependence (\vec{P} is parallel to the z -axis):

$$\frac{\partial B_z}{\partial x}(x, y = 0) = \frac{3\mu_0 x(x^2 - 4z^2)P}{4\pi(x^2 + z^2)^{7/2}}, \quad (3)$$

while the scan data curve, shown in figure 6, can be described by the dependence (\vec{P} is parallel to x -axis)

$$\frac{\partial B_z}{\partial x}(x, y = 0) = \frac{3\mu_0 z(z^2 - 4x^2)P}{4\pi(x^2 + z^2)^{7/2}}. \quad (4)$$

In both cases the baseline of the gradiometer was oriented along the x -axis and the gradiometer plane was placed horizontally parallel to the x, y -plane at height z .

The measurement system described here provided the necessary resolution for fast magnetic particle inspections in construction parts and was easy to operate in a magnetically unshielded laboratory environment. An increase of the gradiometer baseline and an automatic performance of 2D scans at different heights will lead to a better characterization of magnetic particles in future.

The measurement system, in principle, can be applied to determine the distribution of magnetic particles in the sample (see, e.g., [9]). This can be done by recording the 2D magnetic gradient distribution maps followed by a computer deconvolution of the inverse dipole problem. Even in the case of a single dipole, the maps can be interpreted incorrectly without additional information. Additional scans with other

gradiometer orientations are necessary for a solution of the problem.

5. Summary

The combination of the gradiometric configuration of the sensor and a synchronous filtering of the output signal has improved the stability and the resolution of the measurement system in a typical laboratory or industrial environment, where strong magnetic gradients of the line frequency signal due to nearby metallic constructions are usually present. The main requirements for the practical measurement system were fulfilled: the system provided sufficient resolution to detect small magnetic particles in construction parts at a few centimetres distance from the sensor, it has the cryogen hold time of about ten days, and was easy to operate in a magnetically unshielded laboratory environment.

References

- [1] Faley M I, Poppe U, Urban K, Paulson D N, Starr T and Fagaly R L 2001 *IEEE Trans. Appl. Supercond.* **11** 1383–6
- [2] Koch R H, Foglietti V, Rozen J R, Stawiasz K G, Ketchen M B, Lathrop D K, Sun J Z and Gallagher W J 1994 *Appl. Phys. Lett.* **65** 100–2
- [3] Dantsker E, Froehlich O M, Tanaka S, Kouznetsov K, Clarke J, Lu Z, Matijasevic V and Char K 1997 *Appl. Phys. Lett.* **71** 1712–4
- [4] Poppe U, Klein N, Dähne U, Soltner H, Jia C L, Kabius B, Urban K, Lubig A, Schmidt K, Hensen S, Orbach S, Müller G and Piel H 1992 *J. Appl. Phys.* **71** 5572–8
- [5] Faley M I, Poppe U, Urban K, Slobodchikov V Yu, Maslennikov Yu V, Gapelyuk A, Sawitzki B and Schirdewan A 2002 *Appl. Phys. Lett.* **81** 2406–8
- [6] Drung D, Ludwig F, Müller W, Steinhoff U, Trahms L, Koch H, Shen Y Q, Jensen M B, Vase P, Holst T, Freltoft T and Curio G 1996 *Appl. Phys. Lett.* **68** 1421–3
- [7] Varpula T and Poutanen T 1984 *J. Appl. Phys.* **55** 4015–21
- [8] Kasai N, Sasaki K, Kiryu S and Suzuki Y 1993 *Cryogenics* **33** 175–9
- [9] Hohmann R, Lomparski D, Krause H-J, Kreutzbruck M and Hecker W 2001 *IEEE Trans. Appl. Supercond.* **11** 1279–82